Nonenzymatic biomimetic remodeling of phospholipids in synthetic liposomes

Roberto J. Brea[a], Andrew K. Rudd[a], and Neal K. Devaraj[a,1]

[a]Department of Chemistry and Biochemistry, University of California, San Diego, La Jolla, CA 92093

Cell membranes have a vast repertoire of phospholipid species whose structures can be dynamically modified by enzymatic remodeling of acyl chains and polar head groups. Lipid remodeling plays important roles in membrane biology and dysregulation can lead to disease. Although there have been tremendous advances in creating artificial membranes to model the properties of native membranes, a major obstacle has been developing straightforward methods to mimic lipid membrane remodeling. Stable liposomes are typically kinetically trapped and are not prone to exchanging diacylphospholipids. Here, we show that reversible chemoselective reactions can be harnessed to achieve nonenzymatic spontaneous remodeling of phospholipids in synthetic membranes. Our approach relies on transthioesterification/acyl shift reactions that occur spontaneously and reversibly between tertiary amides and thioesters. We demonstrate exchange and remodeling of both lipid acyl chains and head groups. Using our synthetic model system we demonstrate the ability of spontaneous phospholipid remodeling to trigger changes in vesicle spatial organization, composition, and morphology as well as recruit proteins that can affect vesicle curvature. Membranes capable of chemically exchanging lipid fragments could be used to help further understand the specific roles of lipid structure remodeling in biological membranes.

phospholipid | remodeling | native chemical ligation | self-assembly | artificial cell

Living organisms carry out the de novo synthesis of phospholipid membranes, in part, by using membrane-bound acyltransferases and reactive thioester precursors (Fig. 1*A*) (1). Subsequently, de novo synthesized phospholipid membranes can be remodeled by acyltransferases and transacylases in the presence of different lysolipid, phospholipid, and fatty acid precursors (Fig. 1*A*) (2). Such natural mechanisms allow cells to fine-tune properties of biological membranes by changing the composition and organization of their constituent lipids and proteins (3). Membrane remodeling is an essential component of numerous cellular functions including the formation of organelles (4), division (5), trafficking (6), and signaling (7). Many experimental and theoretical studies have examined membrane remodeling due to enzymatically driven changes in lipid composition (8). For instance, the disruption of the transacylase activity of the enzyme tafazzin leads to alterations in the mitochondrial lipid cardiolipin and the disease known as Barth's syndrome (9).

Model membranes composed of well-defined synthetic lipids are useful tools for studying questions related to membrane biology (10, 11). The importance of lipid remodeling in biology underscores the need for straightforward methods to remodel lipid composition in artificial model membranes. Unfortunately, nonenzymatic methods to exchange lysolipid fragments in synthetic vesicles have previously not been feasible. This is likely due to the high kinetic stability of phospholipid membranes, which do not readily exchange diacylphospholipid species between membranes (12). Because the composition of phospholipids controls the physical properties of the resulting membranes, synthetic phospholipid remodeling could be used to gain control over the function and form of artificial membranes, for instance by enabling dynamic changes in vesicle morphology. Here, we demonstrate efficient de novo generation and remodeling of phospholipid vesicles at neutral

pH through application of the native chemical ligation (NCL) (13–18) and reversible native chemical ligation (RNCL) (19) (Fig. 1 *B* and *C* and *SI Appendix*, Figs. S1–S3 and Table S1). Our strategy uses reversible covalent coupling reactions and reactive single-chain lipid precursors, which are known to rapidly exchange between membranes (20). We demonstrate that our protein-free synthetic membranes can be used to test the effects of lipid fragment exchange on membrane properties such as curvature, microdomain formation, and protein recruitment. Advanced model membranes could be harnessed to further understand the effects of chemical lipid remodeling on membrane biology and enable dynamic control over properties of preformed vesicles such as size, shape, and charge.

Results and Discussion

We initially synthesized two substrates to mimic the native precursors of the common phospholipid 1-oleoyl-2-oleoyl-*sn*-glycero-3-phosphocholine (DOPC): an N-methylated cysteine-functionalized analog of the lysolipid 1-oleoyl-sn-glycero-3-phosphocholine (**1**) and a sodium 2-mercaptoethanesulfonate (MESNA) oleoyl thioester **2** in lieu of oleoyl-CoA (Fig. 1 *B* and *C* and *SI Appendix*, Figs. S1 and S2 and Table S1). Precursors **1** and **2** are water-soluble amphiphiles, forming micelles of ~4.5 and 3.8 nm in diameter, respectively, with critical micelle concentrations below 100 µM (for **1**) and 10 µM (for **2**) (*SI Appendix*, Figs. S4 and S5). The high water solubility of both precursors facilitated initial de novo phospholipid synthesis by NCL using mild conditions and millimolar concentrations of lipid precursors. Under typical NCL conditions (NaH$_2$PO$_4$ buffer, pH 7.1, containing DTT as reducing agent), unprotected segment **1** and **2** coupled over 30 min to afford amidophospholipid **3**, a novel phospholipid that resembles DOPC, with the exception of an N-methylated cysteine-amido

Fig. 1. De novo formation and remodeling of phospholipid membrane architecture. (*A*) Enzymatic acyl chain incorporation into membranes during the de novo and remodeling phospholipid synthesis pathways. (*B*) De novo synthesis of phospholipids by NCL reaction of an N-methylated cysteine-functionalized lysolipid (**1**) and MESNA oleoyl thioester (**2**), followed by subsequent remodeling of the corresponding phospholipids by RNCL in the presence of another N-methylated cysteine-functionalized lysolipid (**4**). (*C*) Schematic representation of phospholipid libraries obtained by NCL-based de novo formation and RNCL-based remodeling approaches.

linker (Figs. 1 *B* and *C* and *SI Appendix*, Figs. S1 and S2 and Table S1). Phospholipid formation was analyzed using combined liquid chromatography, MS, and evaporative light scattering detection (ELSD) measurements (*SI Appendix*, Fig. S6).

As expected, neither the N-methylated cysteine-modified lysolipid **1** nor the MESNA thioester **2** formed membranes in aqueous solution. However, the amidophospholipid product **3** readily formed membrane vesicles in situ (*SI Appendix*, Fig. S7 and Movie S1). Lipid vesicular structures were initially identified by fluorescence microscopy using the membrane staining dye Texas Red DHPE (*SI Appendix*, Fig. S8). Confirmation that the resulting structures were

membrane compartments was also achieved by transmission electron microscopy (TEM) (Fig. 2*A* and *SI Appendix*, Fig. S9). In this case, aliquots of the in situ phospholipid samples were collected over 400 mesh Cu/Rh grids, which were then negatively stained with uranyl acetate. Under these conditions, electron microscopy revealed the presence of several populations of spherical vesicles that were between 50–950 nm wide. The efficient in situ encapsulation ability of the vesicles was determined by inclusion of a polar fluorophore, 8-hydroxypyrene-1,3,6-trisulfonic acid (HPTS), in the hydration media, followed by vesicle characterization using fluorescence microscopy (Fig. 2*B* and *SI Appendix*,
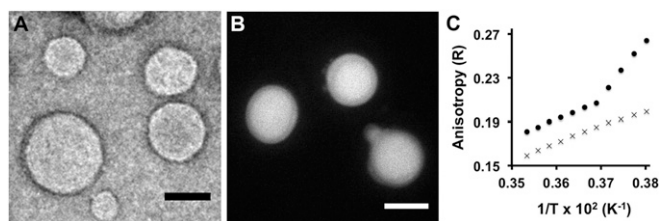
Fig. 2. Characterization of the amidophospholipid vesicular architecture. (*A*) TEM image of negatively stained vesicular structures formed by spontaneous de novo NCL-based synthesis of phospholipid **3**. (Scale bar, 100 nm.) (*B*) Fluorescence microscopy image demonstrating the in situ encapsulation of HPTS within membrane vesicles during de novo synthesis of phospholipid **3**. (Scale bar, 10 μm.) (*C*) Anisotropy of DPH as a function of temperature within membranes formed from phospholipid **3** (×) and **5** (•). A sudden change in the slope of the anisotropy indicates a transition from a gel to liquid-crystalline phase. The melting temperature of the lipid chains in membranes formed from **5** was detected at 270 K, comparable to the transition temperature of analogous POPC membranes. In contrast, within the temperatures tested (263–283 K), a phase transition was not detected in membranes formed from **3**, as predicted by comparing to analogous DOPC membranes (T_c = 256 K). The unitless anisotropy ratio (R) is a measure of the acyl packing of the bilayer, with higher values indicating a more ordered membrane.

Fig. S10). Finally, we determined the gel-to-liquid-phase transition temperature of the resulting membranes by performing steady-state anisotropy measurements as a function of temperature with the membrane fluidity probe 1,6-diphenyl-1,3,5-hexatriene (DPH). The measurements indicate that the amidophospholipid membranes composed from **3** have fluidity and chain melting temperatures comparable to those of native DOPC membranes (T_c = 256 K) (Fig. 2*C* and *SI Appendix*, Figs. S11 and S12).

Using RNCL, we explored the remodeling of amidophospholipid membranes. Initially, we tested the ability of phospholipids to react by RNCL using giant unilamellar vesicles (GUVs) formed by electroformation using interdigitated ITO electrodes (21). This technique allowed for the formation of GUVs (1–100 μm) from amidophospholipid **3** with excellent yield. Confirmation of the lipid vesicular structure was achieved by fluorescence microscopy using the membrane staining dye Bodipy FL DHPE (*SI Appendix*, Fig. S13). GUVs from phospholipid **3** were then used to study the dynamics of the RNCL by following the reaction with N-methylated lysolipids at pH 7.1 in a phosphate buffer containing DTT (*SI Appendix*, Fig. S14). When we combined an aqueous solution of GUVs composed of lipid **3** with 1.0 equivalent of the N-methylated cysteine-functionalized palmitoyl lysolipid **4**, we observed the appearance in the ELSD spectrum of a new peak corresponding to amidophospholipid **5** (*SI Appendix*, Figs. S1 and S14 and Table S1). This confirmed the dynamic covalent character of the RNCL and the ability to remodel **3** to form new phospholipids. Despite their different lipid tail saturation, oleoyl- and palmitoyl-derivatized phospholipids (**3** and **5**, respectively) were present in almost equal concentrations (1:1 ratio), which implies that both species have similar stabilities in the equilibria. Modifications of phospholipid tail saturation can change the physical state of the membrane. Consequently, lipid exchange-based remodeling affords a straightforward approach to modulate the order and fluidity of synthetic phospholipid membranes. As expected, the chain melting temperature for membranes composed of phospholipid **5** was estimated to be 270 K, which is comparable to native 1-palmitoyl-2-oleoyl-*sn*-glycero-3-phosphocholine (POPC) membranes (Fig. 2*C* and *SI Appendix*, Fig. S12). Also, the anisotropy ratio (R) for dyes embedded in membranes formed from phospholipid **5** is higher compared with phospholipid **3**, suggesting that **5** forms more ordered membranes.

We tested whether the equilibria during remodeling could be shifted by using cysteine lysolipids, which irreversibly form stable amide bonds with thioesters. Remodeling of phospholipid membranes spontaneously took place upon the addition of 1.0

equivalent of cysteine-functionalized palmitoyl lysolipid **6** to a solution of GUVs formed from phospholipid **3**, resulting in the appearance of a new peak that corresponded to phospholipid **7** (*SI Appendix*, Figs. S1 and S14 and Table S1). The new phospholipid was the dominant species in the equilibrium, ~30-fold more abundant than the initial N-methylated phospholipid **3**, which at 298 K corresponds to an energy difference of 2.0 kcal·mol⁻¹. It seems likely that the equilibrium is driven by the higher stability of amidophospholipid **7**, which, in the absence of an N-methylated residue avoids the formation of a significant amount of the *cis* isomer, a necessary intermediate for the reversible nonenzymatic process (*SI Appendix*, Fig. S3).

To combine the nonenzymatic de novo and remodeling phospholipid membrane synthesis pathways, we proceeded to study the lipid tail exchange in spontaneously formed vesicles. We initially formed phospholipid **3** by de novo synthesis (Fig. 3*A*, *SI Appendix*, Fig. S7, and Movie S1). Sequential addition of 1.0 equivalent of N-methylated cysteine-functionalized palmitoyl lysolipid **4** to the de novo vesicle population of **3** resulted in lipid remodeling, loss of **1**, and the formation of phospholipid **5**, indicating that RNCL took place (Fig. 3*B* and *SI Appendix*, Figs. S6 and S15). As expected from our previous GUV experiments, the oleoyl- and palmitoyl-derivatized phospholipids (**3** and **5**, respectively) were present in equimolar concentrations (1:1 ratio), demonstrating that both species have analogous stabilities and are in equilibrium. Addition of more than 1.0 equivalent of lysolipid **4** leads to a corresponding shift in the final **3**:**5** lipid ratio, caused by the increase of phospholipid **5** (*SI Appendix*, Fig. S16). This finding suggests that the final phospholipid membrane composition can be controlled through the stoichiometry of the starting reactive lipids. Alternatively, the de novo-formed vesicles of **3** could be irreversibly remodeled by addition of the cysteine-functionalized palmitoyl lysolipid **6**, selectively forming vesicles composed of phospholipid **7** (Fig. 3*C* and *SI Appendix*, Fig. S6).
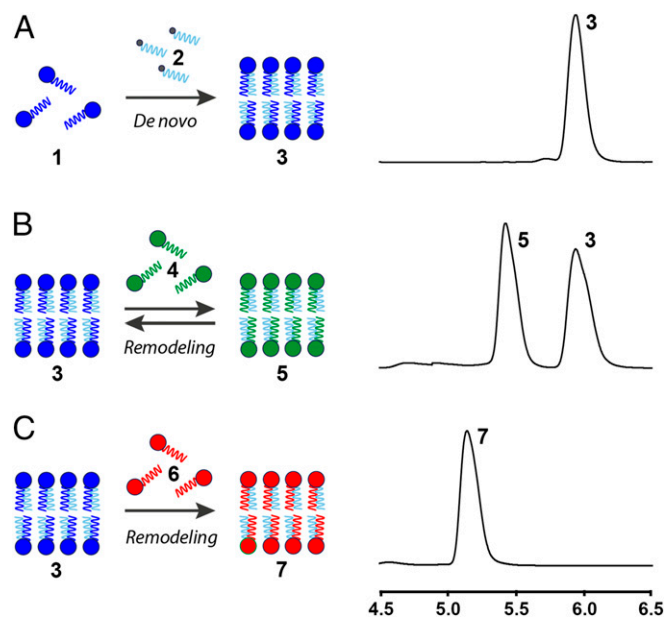
Fig. 3. Sequential de novo phospholipid membrane formation and remodeling driven by nonenzymatic reactions. (*A*) ELSD spectra corresponding to the in situ phospholipid formation of **3**. (*B*) ELSD spectra corresponding to the RNCL exchange reaction between in situ-formed phospholipid **3** and the N-methylated cysteine-functionalized lysolipid **4**, leading to an equimolar mixture of **3** and **5**. (*C*) ELSD spectra corresponding to the RNCL exchange reaction between in situ-formed phospholipid **3** and cysteine-functionalized lysolipid **6**, leading to the selective formation of **7**.

During remodeling, the phospholipid chains can be modulated by changing the reactive precursors (Fig. 1C and *SI Appendix*, Fig. S2). For instance, addition of saturated MESNA thioester **8** to the N-methylated cysteine-based lysolipid **4** led to de novo synthesis of fully saturated amidophospholipid **9** (*SI Appendix*, Figs. S1 and S2 and Table S1). Phospholipid **9** could be remodeled by subsequent addition of N-methylated cysteine-based lysolipid **1** or cysteine lysolipid **6**, affording amidophospholipid **10** or **11**, respectively (*SI Appendix*, Figs. S1 and S2 and Table S1).

Living cells chemically remodel phospholipids to alter larger-scale physical properties of their membranes (2, 3). An important example is the formation of phase-separated compositional lipid microdomains known as "lipid rafts" (22). Lipid rafts have been implicated in a number of important cellular processes including signal transduction (23), membrane trafficking (24), and protein sorting (25), where changes in lipid organization can have a profound impact on the function of membrane proteins. Additionally, lipid raft domains facilitate budding (23), disease states (26), viral assembly (27), and infection (28). Phase transitions in lipid mixtures with the same hydrophilic head are driven by differences in the order state of lipid tails (29, 30). Significantly, the degree of unsaturation in phospholipid tails can change the liquid–gel transition temperature and, therefore, the order state of the chain. With this in mind, we determined whether lipid remodeling of N-methylated amidophospholipids could trigger significant changes in vesicle composition and spatial organization. We used electroformation in the presence of 0.1 mol % of Texas Red DHPE dye to create labeled GUVs containing a mixture of phospholipids **3** and **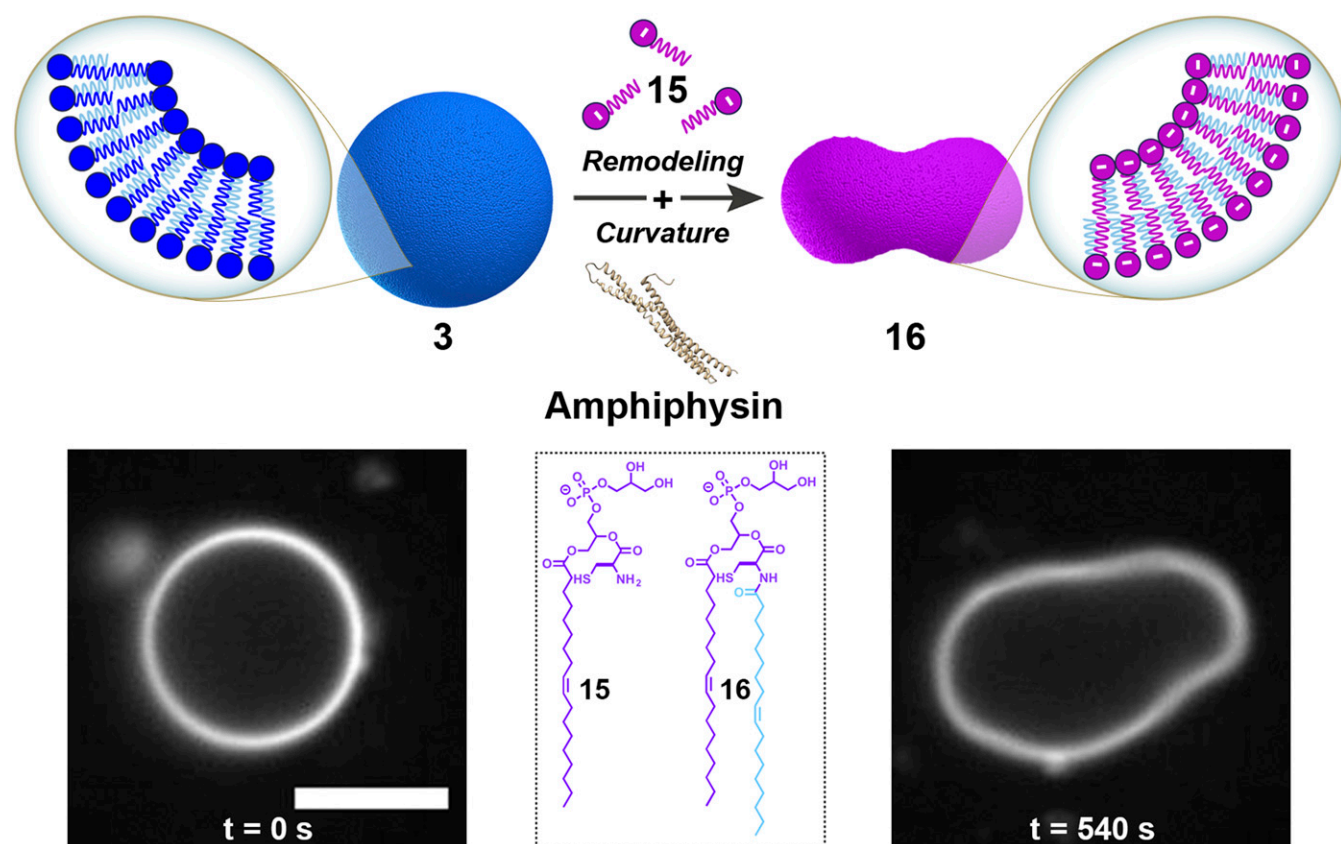10** with cholesterol in a molar ratio of 1:1:0.8. Upon addition of 1.0 equivalent of lysolipid **6**, formation of a new class of GUVs composed of

phospholipids **7**, **11**, and cholesterol was detected. Consequently, a dramatic shift from one miscible phase to two immiscible phases was observed, as indicated by the partitioning of Texas Red DHPE dye into discrete circular regions of the membrane (Fig. 4, *SI Appendix*, and Movie S2). These events occurred within 2–3 min and were apparent in nearly all vesicles observed. Alternatively, microdomain formation was not detected over the same observed period when GUVs composed of **3**, **10**, and cholesterol were treated with the unreactive lysolipid 1-palmitoyl-2-hydroxy-*sn*-glycero-3-phosphocholine (*SI Appendix* and Movie S3). Furthermore, remodeling of the same GUVs by addition of the reactive oleoyl lysolipid **12** (*SI Appendix*, Fig. S1 and Table S1) to generate the phospholipids **13** and **14** (*SI Appendix*, Fig. S1 and Table S1) showed no microdomain formation, suggesting that the presence of fully saturated lipid species is necessary to promote such events (*SI Appendix* and Movie S4). We postulate that lipid microdomains emerge as the composition of the phospholipid membrane shifts to mixtures similar to those known to create two immiscible domains. In situ remodeling of phospholipids by lipid tail exchange leads to subsequent micrometer-scale changes in membrane composition and morphology.

In addition to controlling membrane fluidity, cells are able to modulate their plasmalemma charge through the metabolism of phospholipids bearing different head groups (1, 31). The ability to precisely control membrane charge is crucial for a number of cell functions including signaling (32), lipid trafficking (33), and phagocytosis (31). For instance, during phagocytosis the negative charge of the inner membrane is critical for recruitment and anchoring of proteins required for phagosome formation (31). The subsequent loss of membrane charge, induced by metabolism of negatively charged phospholipids, enables dissociation of membrane-bound

Fig. 4. Lipid microdomain formation induced by RNCL-based remodeling. (*Top*) Schematic representation of microdomain generation directed by membrane remodeling of phospholipid vesicles. GUVs composed of **3**, **10**, and cholesterol (molar ratio of 1:1:0.8) containing 0.1 mol % of Texas Red DHPE dye are remodeled by RNCL exchange reactions with cysteine-functionalized lysolipid **6**, leading to the formation of a new class of GUVs composed of **7**, **11**, and cholesterol. Consequently, a dramatic shift from one miscible phase to two immiscible phases takes place. (*Bottom*) Fluorescence microscopy images tracking membrane remodeling and subsequent microdomain formation driven by the RNCL exchange reactions. An aqueous buffer solution of **3**:**10**:cholesterol GUVs (400 μM) and cysteine-functionalized lysolipid **6** (400 μM) in the presence of DTT (2 mM) was imaged at different times after initial mixing (from 0 to 104 s). Initially, lipid microdomains were not present. However, shortly after the species had been mixed, lipid remodeling took place and microdomain formation was observed, as indicated by the partitioning of Texas Red DHPE dye into discrete circular regions of the membrane. (Scale bar, 10 μm.)

Fig. 5. Membrane curvature induced by RNCL-based remodeling. GUVs composed of neutral phospholipid **3** containing 0.1 mol % of Bodipy FL DHPE dye are remodeled by RNCL exchange reactions with negatively charged lysolipid **15**, leading to the formation of a new class of GUVs composed of **16**. After addition of amphiphysin to the mixture, dramatic membrane curvature events in the negatively charged GUVs of **16** were observed as a result of the protein binding. (Scale bar, 5 μm.)

proteins during phagosome maturation and sealing (31). By using a lysolipid possessing a negatively charged head group, we hypothesized that we could modulate the membrane association of amphiphysin (34, 35), a similar membrane-associated protein. Amphiphysin is a protein involved in endocytosis that is known to bind to negatively charged phospholipid membranes and induce positive curvature in the surface (34). To determine whether remodeling our model membranes could drive similar effects, we first synthesized GUVs composed of neutral N-methylated phosphatidylcholine phospholipid **3** and then added 1.0 equivalent of negatively charged phosphatidylglycerol lysolipid **15** (*SI Appendix*, Figs. S1 and S17*A* and Table S1), observing the formation of a new class of GUVs composed of phosphatidylglycerol phospholipid **16** (*SI Appendix*, Figs. S1, S17*B*, and S18 and Table S1). After reaction completion, amphiphysin (*SI Appendix*, Fig. S19*A*) was subsequently added to the mixture, and dramatic curvature events were observed in the negatively charged GUVs of **16** within 1 min of protein addition (Fig. 5 and *SI Appendix* and Movie S5). This behavior was not observed in phospholipid **3** GUVs before the addition of **15** (*SI Appendix* and Movie S6) or as a result of the remodeling itself (*SI Appendix* and Movie S7), indicating that the change in membrane charge is responsible for the observed protein binding behavior. Analogous remodeling experiments in the presence of the protein epsin 1 (36) (*SI Appendix*, Fig. S19*B*) showed identical membrane curvature events (*SI Appendix*, Fig. S20 and Movie S8). Alternatively, morphological transformations were not detected over the same observed period when controls were carried out (*SI Appendix* and Movies S7 and S9). In addition, treatment of phospholipid **3** GUVs with the neutral oleoyl phosphatidylcholine lysolipid **12** resulted in phospholipid **13** membranes that were not deformed in the presence of amphiphysin (*SI Appendix* and Movie S10) or epsin 1 (*SI Appendix* and Movie S11), suggesting that the membrane remodeling alone is not responsible for protein activity.

Summary and Prospects

In conclusion, we have developed for the first time, to our knowledge, simplified model membranes that mimic how native phospholipid membranes are synthesized and remodeled. The NCL reaction can be efficiently used for the preparation of amidophospholipids that self-assemble in situ to form membrane vesicles. We demonstrate subsequent membrane remodeling directed by the RNCL reaction for the construction of dynamic membranes that can spontaneously change their composition and morphology. Our approach overcomes kinetic barriers to lipid remodeling that are faced with standard liposome preparations. As such, future opportunities could involve exploiting our system to further study the specific effects of lipid remodeling on membrane curvature and organization. Furthermore, our methodology might be harnessed to lower the barrier to changing the size and shape of preformed vesicles in the presence of appropriate stabilizing scaffolds, such as membrane coat proteins (37), provided that N-terminal cysteine residues are absent. The described NCL-based de novo lipid formation and RNCL-based lipid remodeling combined approach should be applicable for studying and exploiting the effects of membrane exchange in minimal model membranes.

1. Holthuis JC, Menon AK (2014) Lipid landscapes and pipelines in membrane homeostasis. *Nature* 510(7503):48–57.
2. Shindou H, Hishikawa D, Harayama T, Yuki K, Shimizu T (2009) Recent progress on acyl CoA: Lysophospholipid acyltransferase research. *J Lipid Res* 50(Suppl):S46–S51.
3. Lipowsky R (2014) Remodeling of membrane compartments: Some consequences of membrane fluidity. *Biol Chem* 395(3):253–274.
4. Cepińska MN, Veenhuis M, van der Klei IJ, Nagotu S (2011) Peroxisome fission is associated with reorganization of specific membrane proteins. *Traffic* 12(7):925–937.
5. Rocha S, et al. (2014) Membrane remodeling processes induced by phospholipase action. *Langmuir* 30(16):4743–4751.
6. Brown WJ, Chambers K, Doody A (2003) Phospholipase A2 (PLA2) enzymes in membrane trafficking: Mediators of membrane shape and function. *Traffic* 4(4):214–221.
7. Vogel V, Sheetz M (2006) Local force and geometry sensing regulate cell functions. *Nat Rev Mol Cell Biol* 7(4):265–275.
8. Jiang Z, de Messieres M, Lee JC (2013) Membrane remodeling by α-synuclein and effects on amyloid formation. *J Am Chem Soc* 135(43):15970–15973.
9. Schlame M, et al. (2012) The physical state of lipid substrates provides transacylation specificity for tafazzin. *Nat Chem Biol* 8(10):862–869.
10. Hanson JM, et al. (2016) Cholesterol-enriched domain formation induced by viral-encoded, membrane-active amphipathic peptide. *Biophys J* 110(1):176–187.
11. Lozano MM, et al. (2013) Colocalization of the ganglioside G(M1) and cholesterol detected by secondary ion mass spectrometry. *J Am Chem Soc* 135(15):5620–5630.
12. McLean LR, Phillips MC (1981) Mechanism of cholesterol and phosphatidylcholine exchange or transfer between unilamellar vesicles. *Biochemistry* 20(10):2893–2900.
13. Vázquez O, Seitz O (2014) Templated native chemical ligation: Peptide chemistry beyond protein synthesis. *J Pept Sci* 20(2):78–86.
14. Raibaut L, Ollivier N, Melnyk O (2012) Sequential native peptide ligation strategies for total chemical protein synthesis. *Chem Soc Rev* 41(21):7001–7015.
15. Dawson PE, Muir TW, Clark-Lewis I, Kent SBH (1994) Synthesis of proteins by native chemical ligation. *Science* 266(5186):776–779.
16. Wieland T, Bokelmann E, Bauer L, Lang HU, Lau H (1953) Über peptidsynthesen. 8. Mitteilung bildung von S-haltigen peptiden durch intramolekulare wanderung von aminoacylresten. *Liebigs Ann Chem* 583(1):129–149.
17. Cole CM, et al. (2015) Spontaneous reconstitution of functional transmembrane proteins during bioorthogonal phospholipid membrane synthesis. *Angew Chem Int Ed Engl* 54(43):12738–12742.
18. Brea RJ, Cole CM, Devaraj NK (2014) In situ vesicle formation by native chemical ligation. *Angew Chem Int Ed Engl* 53(51):14102–14105.
19. Ruff Y, Garavini V, Giuseppone N (2014) Reversible native chemical ligation: A facile access to dynamic covalent peptides. *J Am Chem Soc* 136(17):6333–6339.
20. McLean LR, Phillips MC (1984) Kinetics of phosphatidylcholine and lysophosphatidylcholine exchange between unilamellar vesicles. *Biochemistry* 23(20):4624–4630.
21. Walde P, Cosentino K, Engel H, Stano P (2010) Giant vesicles: Preparations and applications. *ChemBioChem* 11(7):848–865.
22. Fan J, Sammalkorpi M, Haataja M (2010) Formation and regulation of lipid microdomains in cell membranes: Theory, modeling, and speculation. *FEBS Lett* 584(9):1678–1684.
23. Simons K, Gerl MJ (2010) Revitalizing membrane rafts: new tools and insights. *Nat Rev Mol Cell Biol* 11(10):688–699.
24. Hanzal-Bayer MF, Hancock JF (2007) Lipid rafts and membrane traffic. *FEBS Lett* 581(11):2098–2104.
25. de Gassart A, Geminard C, Fevrier B, Raposo G, Vidal M (2003) Lipid raft-associated protein sorting in exosomes. *Blood* 102(13):4336–4344.
26. Michel V, Bakovic M (2007) Lipid rafts in health and disease. *Biol Cell* 99(3):129–140.
27. Chazal N, Gerlier D (2003) Virus entry, assembly, budding, and membrane rafts. *Microbiol Mol Biol Rev* 67(2):226–237.
28. Leser GP, Lamb RA (2005) Influenza virus assembly and budding in raft-derived microdomains: A quantitative analysis of the surface distribution of HA, NA and M2 proteins. *Virology* 342(2):215–227.
29. Veatch SL, Keller SL (2003) Separation of liquid phases in giant vesicles of ternary mixtures of phospholipids and cholesterol. *Biophys J* 85(5):3074–3083.
30. Baumgart T, Hess ST, Webb WW (2003) Imaging coexisting fluid domains in biomembrane models coupling curvature and line tension. *Nature* 425(6960):821–824.
31. Yeung T, Grinstein S (2007) Lipid signaling and the modulation of surface charge during phagocytosis. *Immunol Rev* 219(1):17–36.
32. Shi X, et al. (2013) Ca2+ regulates T-cell receptor activation by modulating the charge property of lipids. *Nature* 493(7430):111–115.
33. Tatsuta T, Scharwey M, Langer T (2014) Mitochondrial lipid trafficking. *Trends Cell Biol* 24(1):44–52.
34. Varkey J, et al. (2010) Membrane curvature induction and tubulation are common features of synucleins and apolipoproteins. *J Biol Chem* 285(42):32486–32493.
35. Peter BJ, et al. (2004) BAR domains as sensors of membrane curvature: The amphiphysin BAR structure. *Science* 303(5657):495–499.
36. Pujals S, et al. (2013) Curvature engineering: Positive membrane curvature induced by epsin N-terminal peptide boosts internalization of octaarginine. *ACS Chem Biol* 8(9):1894–1899.
37. Stagg SM, LaPointe P, Balch WE (2007) Structural design of cage and coat scaffolds that direct membrane traffic. *Curr Opin Struct Biol* 17(2):221–228.